Charge Carrier Transport in Amorphous Organic Semiconductors

by

Benjie Limketkai

Submitted to the Department of Electrical Engineering and Computer Science

in partial fulfillment of the requirements for the degree of

Master of Science in Electrical Engineering and Computer Science

at the

MASSACHUSETTS INSTITUTE OF TECHNOLOGY

September 2003

Author......

Department of Electrical Engineering and Computer Science
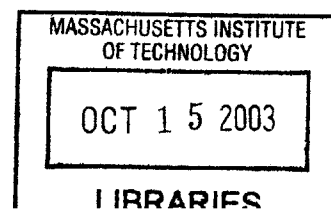
August 29, 2003

Certified by.....

Marc Baldo

Professor

Thesis Supervisor

Accepted by.........

Arthur C. Smith

Chairman, Department Committee on Graduate Student

1

Charge carrier transport in amorphous organic semiconductors

by
Benjie Limketkai

Submitted to the Department of Electrical Engineering and Computer
Science
On August 29, 2003, in partial fulfillment of the
requirement for the degree of
Master of Science in Electrical Engineering and Computer Science

Abstract

Organic semiconductors have been extensively studied ever since the successful fabrication of organic light-emitting diodes (OLED).[42-44] Due to their success, it is becoming increasingly important to understand the theory behind the properties of organic materials. In order to exploit all the advantages of implementing organic materials to construct devices, a detailed understanding of charge-carrier transport in these materials is necessary to obtain optimal efficiency for device operation. In the interface-limited model,[45] transport is heavily dependent on the characteristics of the interface. One important property is the distribution of energy states at the interface. Thin organic films grown from thermal vapor deposition seldom form a smooth interface but rather diverse morphologies. In here, we analyze the effect of the rough metal/organic interface on the density of states, aiding in the study of interface-limited charge transport.

We find that the energy distribution due to the electrostatic potential of the metal/organic charge separation is broad in the interface and gets narrower further into the bulk. Therefore, we have a broad distribution of states at the interface compared to the bulk. Charges are trapped in the tail of the broad density of states and hopping from these interface states into the bulk limits charge transport.

Thesis Supervisor: Marc Baldo
Title: Professor

Acknowledgements

I would like to thank my advisor, Professor Marc Baldo, for his help and guidance with this project and for his wisdom in helping me know what is involved in being a graduate student and ultimately, what is involved to become a good researcher in the science community. I would also like to thank my parents and brothers for their support. I would also like to thank my friends. I am also grateful for the help given by Douglas Lanman and Lakshminarayan Srinivasan. This thesis is dedicated to my parents.

Contents

List of Figures

List of Tables

Chapter 1

Introduction

The research activity for organic semiconductors is increasing due to their potential for many applications. For some devices, thin films of an organic material is used as the active layer. Thin films grown from thermal vapor deposition seldom form a smooth surface but rather assumes diverse morphologies. The roughness of the surface varies depending on the deposition conditions. The structure of the rough surface, and consequently, the physical properties of thin films varies according to the conditions during growth.[1-6] Therefore, it is important for us to understand the possible effects of the rough surface on the properties of the organic semiconductor, and provide a link between the roughness of the surface, characterized by a set of parameters, to the properties of the organic material. Our main interest is to understand how the rough surface may affect charge transport. In order to help facilitate the understanding of charge transport in amorphous organic semiconductors, it is necessary to analyze the physical properties and effects of the structure. We would like to analyze the electrostatic effects of the rough surface formed at the metal-semiconductor contact.

Chapter 2

Rough Surfaces

A thorough explanation of amorphous and crystalline rough surfaces can be found in Ref. 7. For the most part, this section will simply briefly paraphrase necessary background information of rough surfaces from that source.

Most surfaces formed in nature are rough, whether it is the kilometer-scale roughness o f l andscapes o n t he e arth o r t he n anometer-scale r oughness of a n array o f atoms in a structure. The roughness of an interface between two materials is one of the key features in thin film technologies because it directly affects many physical and chemical properties of the films. Examples dependent on interface roughness include the change in the demagnetizing fields and coercivity of thin magnetic films [8,9] and the change in the electrical conductivity of thin metal films.[10] Roughness also affects surface plasmons,[11] surface second-harmonic generation,[12,13] chemical reaction rate,[14] and Brewster angle shifts,[15,16] and etc... Sometimes, the main objective in the analysis of rough surfaces is to help understand its formation in order to eliminate it. Reduction of roughness may be desirable in many thin film applications in microelectronic devices and optoelectronic devices. For example, the roughness of a silicon substrate may affect the gate-oxide quality[17] and the ohmic contact between a metal and a semiconductor.[18] Surface roughness may generate additional scattering losses in optical waveguides.[19] For our purposes, we would like to analyze how the rough surface affects the electrical properties (the potential) in an organic film.

A random rough surface can be mathematically described as $h = h(\vec{r})$, where h is the surface height of a rough surface with respect to a smooth reference surface defined to be the mean surface height and $\vec{r}$ is the position vector on this reference surface. We assume there are no overhangs on the rough surface, hence, the height function h is a single-valued function of the position vector $\vec{r}$. The random rough surface $h(\vec{r})$ is a random field, a random (or stochastic) process with a parameter space that is multidimensional. For a complete description of a random field, one needs to know the n-dimensional joint distribution function $p_n\left(h_1, h_2, ..., h_n; \vec{r_1}, \vec{r_2}, ..., \vec{r_n}\right)$, where $h_1, h_2, ..., h_n$ are the random variables corresponding to the set $\vec{r_1}, \vec{r_2}, ..., \vec{r_n}$ different positions on the surface. We assume the random height field is homogeneous (stationary for a one-dimensional random process). That is, all the joint probability distribution functions are invariant under translation of the locations $\vec{r_1}, \vec{r_2}, ..., \vec{r_n}$ in the parameter space. Hence, the probabilities only depend on the relative locations of $\vec{r_1}, \vec{r_2}, ..., \vec{r_n}$. We also assume that the random height field is isotropic. That is, the joint probability density functions are invariant under rotation of the constellation of points $\vec{r_1}, \vec{r_2}, ..., \vec{r_n}$ in parameter space. Thirdly, we assume that the random height field is ergodic. That is, all the necessary information about the joint distributions and statistics of the random process can be obtained from a single statistical sample realization of the process; therefore, one can use the field average instead of the ensemble average. The ergodic property refers to the equality between the average of one sample waveform and the ensemble average over the sample space of all waveforms comprising the random process.[20] To summarize, our random rough surface is assumed to be a homogeneous, isotropic, ergodic random field.

The height probability density function of the random rough surface is defined to be $p(h)$, where the probability the rough surface has a height between h and $h + dh$ above a point $\vec{r_0}$ on the mean surface plane is $p(h)dh$. The distribution function $p(h)$ is non-negative and normalized such that:

$$\int_{-\infty}^{\infty} p(h)\,dh = 1 \qquad\qquad (2.1)$$

To describe the properties of the random variable $h\left(\vec{r_0}\right)$, the height of the rough surface above the point $\vec{r_0}$, we need to have some numerical statistics which are determined by the distribution function $p(h)$. The nth-order moment of the random variable h is defined as:

$$m_n = E\left[h^n\right] = \int_{-\infty}^{\infty} h^n p(h) dh \tag{2.2}$$

The nth-order central moment of a random variable is defined as:

$$v_n = E\left[\left(h-\overline{h}\right)^n\right] = \int_{-\infty}^{\infty}\left(h-\overline{h}\right)^n p(h) dh \tag{2.3}$$

The expected value operator $E[...]$ is an average operator. It takes the ensemble average of the expression inside the brackets. The first order moment $m_1 = \overline{h}$ is the average height of the rough surface. For realistic rough surface, the average height, or mean, $\overline{h}$ is equal to zero, which implies that $m_n = v_n$. The assumption that $\left\langle h\left(\vec{r}\right)\right\rangle = 0$ ensures that the random field $h\left(\vec{r}\right)$ is homogeneous. The symbol $\left\langle ...\right\rangle$ represents the ensemble average. The second order moment of the random variable h is used to describe the surface roughness:

$$w^2 = m_2 = \int_{-\infty}^{\infty} h^2 p(h) dh, \tag{2.4}$$

where w is called the root-mean-square (rms) roughness or the interface width. Since $\overline{h} = 0$, w is also the standard deviation and w^2 the variance. The rms roughness describes the fluctuations of surface heights around an average surface height, $\overline{h}$. The larger rms roughness, the rougher the surface, given that all other statistical parameters are kept the same. The third order moment of the random variable h defines the skewness of the surface heigh, γ_3, and the fourth order moment defines the kurtosis of the surface height, γ_4. Skewness is a measure of the symmetry of a distribution about a mean surface level, where a positive or negative skewness means that the asymmetric tail extends out above or below the mean surface level, respectively. Kurtosis is a measure of sharpness

10

of the height distribution function. The kurtosis is less for a roughness configuration where m ost o f t he s urface h eights a re concentrated c lose t o t he m ean s urface l evel a s opposed to when most of it is concentrated farther away. Kurtosis describes the randomness of the height profile relative to that of a perfectly random surface (Gaussian distribution) with a kurtosis of 3.0. For $\gamma_4 < 3.0$, the distribution is platykurtic (mild peak). For $\gamma_4 > 3.0$, the distribution is leptokurtic (sharp peak).

The first order statistics related to the height distribution function only describe the statistical properties of the individual random variables at each position of a random field. It does not reflect the connection or correlation between random variables at different positions of the random field. Two rough surfaces may have the same distribution function $p(h)$ and rms roughness w but look very different. The height fluctuation frequencies may be different (the changes in heights occur in different length scales along the surfaces). In order to characterize the spatial difference of a rough surface, we need to discuss the second-order numerical statistics, such as the correlation of a random field $h(\vec{r})$ at two different positions $\vec{r}_1$ and $\vec{r}_2$. Let us define the joint distribution probability density function $p_2(h_1, h_2; \vec{r}_1, \vec{r}_2)$ of the random variables set $\{h(\vec{r}_1), h(\vec{r}_2)\}$. The marginal distributions $p(h_1)$ and $p(h_2)$ of $p_2(h_1, h_2; \vec{r}_1, \vec{r}_2)$ are equal for a homogeneous random field.

$$\int_{-\infty}^{\infty} p_2(h_1, h_2; \vec{r}_1, \vec{r}_2) dh_1 = p(h_2) = p(h)$$

$$\int_{-\infty}^{\infty} p_2(h_1, h_2; \vec{r}_1, \vec{r}_2) dh_2 = p(h_1) = p(h) \qquad (2.5)$$

$$\int_{-\infty}^{\infty} \int_{-\infty}^{\infty} p_2(h_1, h_2; \vec{r}_1, \vec{r}_2) dh_1 dh_2 = 1$$

The joint probability distribution function is related to the correlation between the heights h_1 and h_2 at the two different positions $\vec{r}_1$ and $\vec{r}_2$. If the two random variables h_1 and h_2 are independent of each other, then $p_2(h_1, h_2; \vec{r}_1, \vec{r}_2) = p(h_1) p(h_2)$ and h_1 and h_2

11

are said to be uncorrelated. Now, we define the second-order statistics related to the joint distribution. The autocovariance function $G\left(\vec{r_1}, \vec{r_2}\right)$ is defined as:

$$G\left(\vec{r_1}, \vec{r_2}\right) = E\left[h\left(\vec{r_1}\right)h\left(\vec{r_2}\right)\right] = \int\limits_{-\infty}^{\infty}\int\limits_{-\infty}^{\infty} h_1 h_2 p_2\left(h_1, h_1; \vec{r_1}, \vec{r_2}\right)dh_1 dh_2 \qquad (2.6)$$

The autocorrelation function $R\left(\vec{r_1}, \vec{r_2}\right)$ is related to the autocovariance function $G\left(\vec{r_1}, \vec{r_2}\right)$ by:

$$R\left(\vec{r_1}, \vec{r_2}\right) = \frac{G\left(\vec{r_1}, \vec{r_2}\right)}{w^2} \qquad (2.7)$$

The autocorrelation and autocovariance functions give us some statistics on the correlation of the heights at two positions $\vec{r_1}$ and $\vec{r_2}$. Since we assume our rough random field surface is homogeneous and isotropic, $R\left(\vec{r_1}, \vec{r_2}\right)$ and $G\left(\vec{r_1}, \vec{r_2}\right)$ will only depend on the relative positions of $\vec{r_1}$ and $\vec{r_2}$:

$$\begin{aligned} G\left(\vec{r_1}, \vec{r_2}\right) &= G\left(\left|\vec{r_1} - \vec{r_2}\right|\right) = G(\rho) \\ R\left(\vec{r_1}, \vec{r_2}\right) &= R\left(\left|\vec{r_1} - \vec{r_2}\right|\right) = R(\rho) \end{aligned} \qquad (2.8)$$

The difference between the two positions $\vec{r_1}$ and $\vec{r_2}$, ρ, is sometimes referred to as the lag or slip. The autocovariance function at zero lag ($\rho = 0$) is equal to the interface width squared, or the variance.

$$G(0) = G\left(\left|\vec{r} - \vec{r}\right|\right) = G\left(\vec{r}, \vec{r}\right) = E\left[h\left(\vec{r}\right)h\left(\vec{r}\right)\right] = \int\limits_{-\infty}^{\infty} h^2 p(h)dh = w^2 \qquad (2.9)$$

Correlation length, or lateral correlation length, ξ is defined as the lag at which the value of the autocorrelation function drops by a factor of $\dfrac{1}{e}$ of its zero lag value $R(0) = 1$, ie, $R(\xi) = \dfrac{1}{e}$. The correlation length represents the maximum distance between two points $\vec{r_1}$ and $\vec{r_2}$ on a rough surface where the heights $h\left(\vec{r_1}\right)$ and $h\left(\vec{r_2}\right)$ are still

12

considered to be correlated. Note, for $\rho \gg \xi$, the two heights at two points separated by a distance ρ are not correlated and hence independent of each other, $\lim_{\rho \to \infty} R(\rho) = 0$.

We can also define the height difference correlation function, or sometimes called the height-height correlation or structure function, $H(\vec{\rho})$:

$$H(\vec{\rho}) = E\left[\left\{h(\vec{r}) - h(\vec{r} + \vec{\rho})\right\}^2\right] = 2w^2\left(1 - R(\vec{\rho})\right) \qquad (2.10)$$

For homogeneous and isotropic random surface, the height difference correlation function only depends on the magnitude $|\vec{\rho}|$.

As a consequence of the Wiener-Khintchine theorem,[20] the power spectrum $P(\vec{k})$ is the fourier transform of the autocovariance function $G(\vec{\rho})$:

$$P(\vec{k}) = \frac{1}{2\pi} \int_{-\infty}^{\infty} G(\vec{\rho}) e^{i\vec{k}\cdot\vec{\rho}} d\vec{k}, \qquad (2.11)$$

where $\vec{k}$ is the wave vector in fourier (reciprocal) space. For a homogeneous and isotropic random field, the power spectrum only depends on the magnitude of the wave vector $|\vec{k}|$. Note that the average power is equal to the variance:

$$\overline{P} = \int_{-\infty}^{\infty} P(\vec{k}) d\vec{k} = G(0) = w^2 \qquad (2.12)$$

It can be shown that the random field representing the random rough surface is continuous, differentiable, and has local integrals in the mean-square sense.[7,21]

So far, we have discussed how to represent random rough surface as a random field and how to characterize it with some statistical parameters. These were merely general mathematical tools for random processes. We have not yet presented a particular model or function to depict the rough surface. In here, we will use a self-affine model to represent the surface morphology of organic thin films.

A self-affine scaling model is very useful for describing a wide variety of rough surfaces.[6] This model is based on fractals, which have the property of invariance under a scale change. A self-similar fractal object is invariant under a similarity transformation. That is, the object exhibits scale invariance and looks statistically the same even though

the scale is stretched uniformly by a factor of ε. A self-affine fractal object looks the same under an affine transformation. That is, the object looks statistically the same even though the scale is stretched with different factors in different directions.

A rough surface that is described by a single-valued self-affine function has the following property:[22]

$$h\left(x_1, x_2, ..., x_n\right) = \varepsilon_1^{-\alpha_1} \varepsilon_2^{-\alpha_2} ... \varepsilon_n^{-\alpha_n} h\left(\varepsilon_1 x_1, \varepsilon_2 x_2, ..., \varepsilon_n x_n\right) \tag{2.13}$$

where h is the surface height at a point in n-dimensions and α_i are the roughness or Hurst exponents. For one characteristic roughness exponent, we obtain $h(x) = \varepsilon^{-\alpha} h(\varepsilon x)$.

The self-affine surface is a fractal object that can be characterized by a roughness exponent that is related to the fractal dimension of the surface D_S and the dimension of the embedded space d by $d + 1 - D_S$. The roughness exponent ($0 \le \alpha \le 1$) is a parameter that shows how jagged the rough surface is. A small or large value of α correspond to a relatively jagged or smooth surface structure at a scale less than ξ, respectively. The height difference correlation function of a self-affine surface has the form:[22-25]

$$H\left(\vec{r} - \vec{r}'\right) = \left\langle \left[h\left(\vec{r}\right) - h\left(\vec{r}'\right)\right]^2 \right\rangle = H(\rho) = 2w^2 f\left(\frac{\rho}{\xi}\right) \tag{2.14}$$

where $f(x)$ is a scaling function having the asymptotic property,

$$f(x) = \begin{cases} x^{2\alpha}, & for\ x \ll 1 \\ 1, & for\ x \gg 1 \end{cases} \tag{2.15}$$

Hence, the height difference correlation function has the following asymptotic form:[7]

$$H(\rho) = \begin{cases} w^2 \left(\frac{\rho}{\xi}\right)^{2\alpha}, & for\ \rho \ll \xi, \\ 2w^2, & for\ \rho \gg \xi \end{cases} \tag{2.16}$$

where ξ is the correlation length and w is the interface width. The power spectrum of a self-affine surface has the form:

$$P(k) = w^2 g(\xi k), \tag{2.17}$$

where the function $g(x)$ is a scaling function having the asymptotic property,

$$g(x) = \begin{cases} 1, & \text{for } x \ll 1 \\ x^{-2\alpha-d}, & \text{for } x \gg 1 \end{cases} \tag{2.18}$$

where d is the dimension of the embedded space and α is the roughness exponent. The power spectrum has the following asymptotic form:

$$P(k) = \begin{cases} w^2, & \text{for } \xi k \ll 1 \\ w^2 (\xi k)^{-2\alpha-d}, & \text{for } \xi k \gg 1 \end{cases} \tag{2.19}$$

Chapter 3

Self-Affine Roughness Model

We will use the self-affine surface roughness model for our rough surface/interface. Our random rough surface can be mathematically represented as a single-valued random field height function $h(\vec{r})$ with respect to a mean surface $\langle h(\vec{r}) \rangle$, where $\vec{r}$ is the in-plane positional vector of this mean surface. We assume our random rough surface $h(\vec{r})$ is homogeneous, isotropic, and ergodic. We define $P(k)$, the roughness spectrum, to be the fourier transform of the height-height autocorrelation function $R(\vec{r}) = \langle h(\vec{r}) h(0) \rangle$, where $\langle h \rangle$ is defined to be zero. Since our random surface field is homogeneous and isotropic, $P(k)$ will only be a function of the magnitude $|\vec{k}|$ and the $R(\vec{r})$ will only be a function of the position difference ρ. For self-affine surfaces, $P(k)$ scales as a power-law:

$$P(k) = \begin{cases} w^2, & \textit{for } \xi k \ll 1 \\ w^2 (\xi k)^{-2\alpha-2}, & \textit{for } \xi k \gg 1 \end{cases}, \tag{3.1}$$

where w is the interface width or rms roughness (second order moment of the height function h, which is also equal to the standard deviation because $\langle h \rangle = 0$), k is the

magnitude of the wave vector, α is the roughness exponent, and ξ is the correlation length defined as the lag length value at which the autocorrelation function $G(\vec{r})$ drops by a factor of $\dfrac{1}{e}$ of its zero lag value $G(0)$.

We need a uniform theoretical expression for the roughness spectrum function for our self-affine fractal surface. The function we will use for the roughness spectrum that satisfies the scaling behavior is given by the k-correlation model.[26] This model has been used for many rough surface studies.[27-34] From the k-correlation model, the roughness spectrum is:

$$P(k) = \frac{1}{2\pi} \frac{w^2 \xi^2}{\left(1 + ak^2\xi^2\right)^{1+H}}, \tag{3.2}$$

where a is a parameter determined by the normalization condition:

$$\overline{P} = \int\limits_{0<k<k_c} P(k)\,d\vec{k} = G(0) = w^2 \tag{3.3}$$

where $k_C = \dfrac{\pi}{a_0}$ is the upper cutoff frequency and a_0 is the lattice spacing of the atoms. We do not expect any fractal behavior at the atomic level, so the integration limit is at the frequency cutoff k_C. Therefore, a is given by:

$$a = \begin{cases} \dfrac{1}{2\alpha}\left[1 - \left(1 + ak_c^2\xi^2\right)^{-\alpha}\right], & 0 < \alpha < 1 \\[3mm] \dfrac{1}{2}\ln\left[1 + ak_c^2\xi^2\right], & \alpha \to 0 \end{cases} \tag{3.4}$$

For $\alpha > 0$ and $a_0 \ll \xi$, we can approximate the parameter, $a \approx \dfrac{1}{2\alpha}$, which gives the following expression for the roughness spectrum:

$$P(k) = \frac{1}{2\pi} \frac{w^2 \xi^2}{\left(1 + \dfrac{k^2\xi^2}{2\alpha}\right)^{1+\alpha}} \tag{3.5}$$

Chapter 4

Poisson Equation

In order to solve for the potential field in the organic material, we need to introduce Poisson's equation. We will follow the derivation of necessary and informative background information from Ref. 35.

Poisson's equation is given by:

$$\nabla^2 \Phi\left(\vec{r}\right) = \frac{-\rho\left(\vec{r}\right)}{\varepsilon}.\tag{4.1}$$

In order to solve for the potential $\Phi\left(\vec{r}\right)$, where $\vec{r}$ is a positional vector in space, we need to have some boundary conditions. However, it is necessary to know what kind of boundary conditions are appropriate for Poisson's equation to ensure that the solution will be unique and well-behaved inside this boundary region. The type of boundary conditions we will be using for our analysis are the Dirichlet boundary conditions, ie, the potential is specified at the boundaries of the closed region.

We want to show that if we find a solution for a Dirichlet problem, then that solution is the only solution. We will prove uniqueness by contradiction. Suppose that there exist two solutions Φ_1 and Φ_2 that satisfy Poisson's equation and the boundary conditions at S surrounding the region R. Let $U = \Phi_1 - \Phi_2$, then $\nabla^2 U = 0$ in R and U=0 at S. From Green's first identity, we find:[35]

$$\int_V \left(U\nabla^2 U + \nabla U \cdot \nabla U \right) d\vec{x} = \oint_S U \frac{\partial U}{\partial n} da \quad \Leftrightarrow \quad \int_V |\nabla U|^2 d\vec{x} = 0 \qquad (4.2)$$

Therefore, $\nabla U = 0$, which implies that U is constant in R. Since $U = 0$ on S, this means that $U = 0$ in R; in other words, the solution is unique, $\Phi_1 = \Phi_2$.

Now that we have Poisson's equation, we would like to somehow utilize it to formulate our problem. We want to solve Poisson's equation, but we will need to know how the charges are distributed in the region of interest, i.e., find an expression for $\rho(\vec{r})$ in the space the organic material occupies. In our semiconductor, the charge density is:

$$\rho(\vec{r}) = q\left[N_D - n(\vec{r}) \right], \qquad (4.3)$$

where q is the elementary charge, N_D is the density of organic molecules independent of position, and n is the concentration of electrons. We assume that the electrons in the LUMO level of the organic molecules are capable of eventually moving in a way to maintain equilibrium. The expression used for the charge density of the electrons influenced by the potential present in the organic medium follows a Boltzmann distribution:

$$n(\vec{r}) = N_D e^{\frac{q\Phi(\vec{r})}{kT}}, \qquad (4.4)$$

where k is Boltzmann's constant, T is the temperature, and the potential $\Phi(\vec{r})$ is chosen to be equal to zero at infinity (far into the bulk of the organic semiconductor). Substituting the charge density into Poisson's equation, we obtain the Poisson-Boltzmann equation:

$$\nabla^2 \Phi = \frac{-qN_D}{\varepsilon} \left(1 - e^{\frac{q\Phi}{kT}} \right) \qquad (4.5)$$

For our boundaries, we will treat the metal side of the metal/organic junction as a half plane boundary and the other boundary to be at infinity past the half plane. The potential will be specified to be zero at infinity and V_0 at the metal boundary, where we

19

assume that the metal is a perfect conductor so that the potential is constant throughout the conductor. The potential V_0 is the measured built-in voltage plus any applied external voltage. The built-in potential arises because when the metal and organic are brought together into contact, there will be a transfer of charges (electrons moving from the organic to rest on the metal surface to form a surface charge density) to maintain equilibrium of the Fermi level. This displacement of charges will create a built-in potential V_0 measured at the metal with respect to deep inside the organic semiconductor (defined to be zero potential). A depletion region near the junction will be primarily occupied by positively charged molecules due to uncompensated electrons displacing to the metal side.

Equation 4.5 is non-linear, but it will be easier to solve if we make some approximations. For large potential, the exponential term on the right hand side can be assumed to be zero. This is true if we're near the junction and V_0 is large enough. For a - 1 volt built-in potential and at room temperature, the exponential term is very small $\approx 1.6 \times 10^{-17}$ at the junction. We can approximate asymptotically near the junction, but we will need to introduce another boundary condition since a zero potential at infinity will not be able to be satisfied. Hence, we use the full depletion approximation, which assumes that the organic semiconductor is fully depleted in the depletion region. This assumes that all the organic molecules within this depletion region of width z_d have uncompensated electrons that displaced themselves towards the metal surface. This method has been used in many textbooks,[36] and it gives a reasonable approximation for the potential in the semiconductor.

In the full depletion approximation, the charge density is basically a step function. Let us define $z = 0$ to be the metal/semiconductor junction and $z = z_d$ to be the edge of the depletion region. We can neglect the exponential term and our charge density becomes:

$$\rho\left(\vec{r}\right) = \begin{cases} qN_D, & for\ 0 \le z \le z_d \\ 0, & for\ z_d \le z \end{cases} \tag{4.6}$$

Assuming first that our metal/semiconductor junction is flat, the Poisson-Boltzmann equation with boundary conditions is now:

$$\begin{cases} \nabla^2\Phi = \dfrac{-qN_D}{\varepsilon} \\ \Phi(x,y,0) = V_0 \\ \Phi(x,y,z_d) = 0 \end{cases} \qquad (4.7)$$

Equations 4.7 is for the potential in the region $0 \le z \le z_d$. The potential for $z > z_d$ is zero. We've split up the region into two parts. The first region is the depletion region, where the potential is solved from equations 4.7, and the second region is to the right of the depletion region, where the potential is zero. Solving the second-order linear constant coefficients ordinary differential equation, we get a general solution, which is the sum of the homogenous and particular solutions:

$$\Phi = c_1 z + c_2 - \frac{qN_D}{2\varepsilon} z^2 \qquad (4.8)$$

Applying our boundary conditions, we can solve for the constants:

$$\Phi = \left[\left(\frac{qN_D}{2\varepsilon} \right) z_d - \frac{V_0}{z_d} \right] z + V_0 - \frac{qN_D}{2\varepsilon} z^2 \qquad (4.9)$$

Since the electric field is equal to the negative gradient of the potential, we find:

$$E = \frac{qN_D}{\varepsilon} z - \left[\left(\frac{qN_D}{2\varepsilon} \right) z_d - \frac{V_0}{z_d} \right] \qquad (4.10)$$

From Gauss' law, we know that the electric field at $z = z_d$ is zero and the field at $z = 0$ is equal to the total charge in the semiconductor (with the full depletion approximation, the total charge in the depletion region). Using one of these boundary conditions for the electric field gives us the expression for the depletion width:

$$z_d = \sqrt{\frac{-2\varepsilon V_0}{qN_D}}. \qquad (4.11)$$

Note that V_0 is negative relative to the bulk potential, so z_d is a real number. Substituting the expression for the depletion width into the equation for the potential:

$$\Phi = -\left(\frac{qN_D}{2\varepsilon} \right)(z_d - z)^2 \qquad (4.12)$$

This solution for the potential obtained from the full depletion method approximates the numerical solution well near the junction and in the depletion region.

However, if we want to know the potential very near the depletion layer edge or far away deep into the semiconductor, then we will need to do another approximation. In the region past the depletion layer, we have small potential and therefore, we can replace the exponential term in the Poisson equation with:

$$e^{\frac{q\Phi}{kT}} \approx 1 + \frac{q\Phi}{kT} \tag{4.13}$$

Poisson-Boltzmann equation is now:

$$\begin{cases} \nabla^2\Phi = \dfrac{q^2 N_D}{\varepsilon kT}\Phi \\ \Phi(x,y,z \to \infty) = 0 \end{cases} \tag{4.14}$$

Solving the differential equation and matching to the other asymptotic approximation for large potential:

$$\Phi = V_0 e^{-\sqrt{\frac{q^2 N_D}{\varepsilon kT}}z} \tag{4.15}$$

We've s olved f or t he p otential n ear a nd far a way from t he j unction (large a nd small potential, respectively) for a flat surface. In the next section, we will solve for the potential for a rough surface junction/interface.

Chapter 5

Electrostatic Analysis of Rough Metal/Organic Junction

We want to study the effect of the rough interface at the metal/organic junction on the field and hence, the energy, in the organic. Let us choose the coordinate system to have the z-axis to point towards the bulk of the organic semiconductor and the $z = 0$ plane equal to the mean surface of the rough interface. Representing the rough metal/organic interface as a random height field $h(x,y)$ with $\langle h(x,y)\rangle = 0$, our boundary value problem is:

$$
\begin{cases}
\nabla^2 \Phi = \dfrac{-qN_D}{\varepsilon}\left(1 - e^{\frac{q\Phi}{kT}}\right) \\
\Phi\left(x,y,z = h(x,y)\right) = V_0 \\
\quad \Phi\left(x,y,z \to \infty\right) = 0
\end{cases}
\qquad (5.1)
$$

Let us first find the potential near the junction. Using the full-depletion approximation, we have to solve the Poisson-Boltzmann equation with the following boundary conditions:

23

$$\begin{cases} \nabla^2 \Phi = \dfrac{-qN_D}{\varepsilon} \\ \Phi\big(x,y,z=h(x,y)\big) = V_0 , \\ \Phi\big(x,y,z=d(x,y)\big) = 0 \end{cases}$$ (5.2)

where from Gauss' Law, $d(x,y) = z_d + \lambda h(x,y)$ is the rough depletion edge with $z_d = \langle d(x,y) \rangle$ as the mean depletion width and λ is a factor that relates the depletion edge to the rough interface. The mean depletion width z_d for the rough interface case is equal to the depletion width for the flat interface case. Expanding the boundary conditions:

$$\Phi\big(x,y,z=h(x,y)\big) = \sum_{n=0}^{\infty} h^n \frac{\Phi^{(n)}(0)}{n!}$$

$$\Phi\big(x,y,z=d(x,y)\big) = \sum_{n=0}^{\infty} (\lambda h)^n \frac{\Phi^{(n)}(z_D)}{n!}$$ (5.3)

If we assume that our interface is not very rough (the rms roughness is small enough), we will be able to expand our solution Φ using perturbation methods.[28,37-40] We pick the variance of the rough surface w^2 to be our perturbation parameter and expand the solution in powers of $\in = w^2$:

$$\Phi(r) = \Phi_0(r) + \in \Phi_1(r)$$ (5.4)

The equations for order $\in^0$:

$$\begin{cases} \nabla^2 \Phi_0 = \dfrac{-qN_D}{\varepsilon} \\ \Phi_0(x,y,0) = V_0 \\ \Phi_0(x,y,z_d) = 0 \end{cases}$$ (5.5)

The equations for order $\in^1$:

$$\begin{cases} \nabla^2 \Phi_1 = 0 \\[2mm] \Phi_1(x,y,0) = -\left(\dfrac{h}{w^2}\right)\dfrac{d\Phi_0}{dz}\bigg|_{z=0} \\[3mm] \Phi_1(x,y,z_d) = -\lambda\left(\dfrac{h}{w^2}\right)\dfrac{d\Phi_0}{dz}\bigg|_{z=z_d} \end{cases} \qquad (5.6)$$

The solution for Φ_0 is simply the solution for a flat surface metal/semiconductor junction from equation 4.12:

$$\Phi_0 = -\left(\frac{qN_D}{2\varepsilon}\right)(z_d - z)^2 , \; where \; z_d = \sqrt{\frac{-2\varepsilon V_0}{qN_D}} . \qquad (5.7)$$

To begin solving equations 5.6, we transform the Cartesian (x,y) space to the Fourier domain (k_x, k_y):

$$\begin{cases} \left(\dfrac{d^2}{dz^2} - K^2\right)\Phi_1 = 0 \\[3mm] \Phi_1\left(\vec{k},0\right) = -h\left(\vec{k}\right)\dfrac{d\Phi_0}{dz}\bigg|_{z=0} = -\dfrac{1}{w^2}h\left(\vec{k}\right)\left[\dfrac{qN_D}{\varepsilon}z_d\right], \\[3mm] \Phi_1\left(\vec{k},z_d\right) = -\dfrac{\lambda}{w^2}h\left(\vec{k}\right)\dfrac{d\Phi_0}{dz}\bigg|_{z=z_d} = 0 \end{cases} \qquad (5.8)$$

where $\vec{k} = \left(k_x, k_y\right)$ is the wave vector in the lateral direction of $\hat{z}$ and $K^2 = k_x^2 + k_y^2$ is the magnitude squared of the wave vector. Solving the differential equation:

$$\Phi_1\left(\vec{k},z\right) = A\left(\vec{k}\right)e^{Kz} + B\left(\vec{k}\right)e^{-Kz} \qquad (5.9)$$

Applying the boundary conditions, we find:

$$\Phi_1\left(\vec{k},z\right) = \frac{1}{w^2}h\left(\vec{k}\right)\left(\frac{qN_D}{\varepsilon}z_d\right)\left[\frac{\sinh\left(K\left(z-z_d\right)\right)}{\sinh\left(Kz_d\right)}\right]. \qquad (5.10)$$

The solution for Φ_1 is the first order correction term to reflect how a rough surface potential solution deviates from a flat surface solution.

25

We have a solution for the potential near the junction. Let us now find the potential near the depletion layer edge and deeper into the semiconductor. Therefore, our boundary-value problem becomes:

$$
\begin{cases}
\nabla^2 \Phi = \dfrac{q^2 N_D}{\varepsilon kT} \Phi \\
\Phi\left(x, y, z = h(x, y)\right) = V_0, \\
\Phi\left(x, y, z \to \infty\right) = 0
\end{cases}
\tag{5.11}
$$

We've added a boundary condition at the metal surface even though the potential at the surface is too large to agree with the small potential approximation. Adding a boundary condition at the metal boundary will give us the same solution as equation 4.15 for a flat surface. The solution we obtain will only be valid for the region past the depletion layer. Expanding the boundary conditions:

$$
\Phi\left(x, y, z = h(x, y)\right) = \sum_{n=0}^{\infty} h^n \frac{\Phi^{(n)}(0)}{n!}
\tag{5.12}
$$

$$
\Phi\left(x, y, z \to \infty\right) = 0
$$

Similarly to the near junction potential solution, we expand the small potential solution in powers of $\epsilon = w^2$:

$$
\Phi(r) = \Phi_0(r) + \epsilon\, \Phi_1(r)
\tag{5.13}
$$

The equations for order ϵ^0:

$$
\begin{cases}
\nabla^2 \Phi_0 = \dfrac{-q^2 N_D}{\varepsilon kT} \Phi_0 \\
\Phi_0\left(x, y, 0\right) = V_0 \\
\Phi_0\left(x, y, z \to \infty\right) = 0
\end{cases}
\tag{5.14}
$$

The equations for order ϵ^1:

$$
\begin{cases}
\nabla^2 \Phi_1 = 0 \\
\Phi_1\left(x, y, 0\right) = -\left(\dfrac{h}{w^2}\right)\dfrac{d\Phi_0}{dz}\bigg|_{z=0} \\
\Phi_1\left(x, y, z \to \infty\right) = 0
\end{cases}
\tag{5.15}
$$

26

The solution for Φ_0 is simply the solution for a flat surface metal/semiconductor junction from equation 4.15:

$$\Phi_0 = V_0 e^{-\sqrt{\frac{q^2 N_D}{\varepsilon kT}}z} . \tag{5.16}$$

To begin solving equation 5.15, we transform the Cartesian (x, y) space to the Fourier domain (k_x, k_y):

$$\begin{cases} \left(\dfrac{d^2}{dz^2} - K^2 - \dfrac{q^2 N_D}{\varepsilon kT} \right) \Phi_1 = 0 \\[2mm] \Phi_1(\vec{k}, 0) = -\dfrac{1}{w^2} h(\vec{k}) \dfrac{d\Phi_0}{dz} \bigg|_{z=0} = h(\vec{k}) \left[V_0 \sqrt{\dfrac{q^2 N_D}{\varepsilon kT}} \right], \\[2mm] \Phi_1(\vec{k}, z \to \infty) = 0 \end{cases} \tag{5.17}$$

where $\vec{k} = (k_x, k_y)$ is the wave vector in the lateral direction of $\hat{z}$ and $K^2 = k_x^2 + k_y^2$ is the magnitude squared of the wave vector. Solving the differential equation:

$$\Phi_1(\vec{k}, z) = A(\vec{k}) e^{\sqrt{K^2 + \frac{q^2 N_D}{\varepsilon kT}}z} + B(\vec{k}) e^{-\sqrt{K^2 + \frac{q^2 N_D}{\varepsilon kT}}z} \tag{5.18}$$

Applying the boundary conditions, we find:

$$\Phi_1(\vec{k}, z) = \frac{1}{w^2} h(\vec{k}) \left(V_0 \sqrt{\frac{q^2 N_D}{\varepsilon kT}} \right) e^{-\sqrt{K^2 + \frac{q^2 N_D}{\varepsilon kT}}z} . \tag{5.19}$$

The solution for Φ_1 is the first order correction term reflecting how a rough surface potential solution deviates from a flat surface solution.

We have found expressions for the potential in the organic near the junction and far away from the depletion edge. The built-in potential in the semiconductor, created by the displacement of electrons from the organic to the metal, is related to energy by a factor of q. Therefore, the mean energy of the electrostatic potential is:

$$\langle E \rangle = q \cdot E[\Phi_0 + \in \Phi_1] = q \cdot \{ E[\Phi_0] + E[\in \Phi_1] \} \tag{5.20}$$

27

The first term on the right hand side of equation 5.20 is equal to Φ_0 because it is not a function of a random process. However, the second term has the random process field $h(\cdot)$ in the expression for Φ_1.

A random process $x(\cdot)$ is wide-sense stationary if its mean is a constant and its autocorrelation function is a function of the time difference only (it depends only on the relative position of the constellation points, not the absolute positions).[41] Note that a wide-sense stationary random process input $x(t)$ to a system with a transfer function $h(t)$ will have an output $y(t)$ that is also wide-sense stationary. The mean of the output $y(t)$ is equal to:[41]

$$E\big[y(t)\big] = E\big[X(f)H(f)\big] = \mu_X H(0),\qquad(5.21)$$

where μ_X is the mean of the random process $x(t)$ and $H(f)$ is the frequency response of the system. Let $R_X(\rho)$ be the autocorrelation of $x(t)$. It is only a function of the time difference ρ because that is one of the properties of a wide sense stationary process. The autocorrelation of the output of the system with input $x(t)$ will be:[41]

$$R_Y(\rho) = R_X(\rho) * h(\rho) * h(-\rho)\qquad(5.22)$$

$$\Leftrightarrow S_Y(f) = S_X(f)\big|H(f)\big|^2\qquad(5.23)$$

where $S_X(f)$ and $S_Y(f)$ are the power spectral densities of $x(t)$ and $y(t)$, respectively.

Since our random height field $h(x,y)$ is wide-sense stationary and following equation 5.21, the mean of Φ_1 will be zero. Therefore, the mean energy near the junction as a function of z is:

$$\langle E\rangle = q\cdot\big\{E[\Phi_0] + E[\in\Phi_1]\big\} = q\cdot\left[-\left(\frac{qN_D}{2\varepsilon}\right)(z_d - z)^2\right]\qquad(5.24)$$

We want to calculate the variance in energy in a plane $z = z_0$, a layer positioned at z_0 in the organic. The flat-surface potential Φ_0 will not contribute to the variance

28

because it's not a function of a random process. Therefore, the variance in the tangential plane as a function of z near the junction will be:

$$Var[E] = q \cdot Var[\in \Phi_1] = q \cdot G_{\in\Phi_1}(0) = q \cdot \int_{0<|\vec{k}|<k_C} P_{\in\Phi_1}(\vec{k}) d\vec{k} \qquad (5.25)$$

From equation 5.23, the power spectrum of Φ_1 is:

$$P_{\in\Phi_1}(\vec{k}) = P_h(\vec{k}) \cdot \left| \left(\frac{qN_D}{\varepsilon} z_D \right) \frac{\sinh(K(z-z_D))}{\sinh(Kz_D)} \right|^2 \qquad (5.26)$$

The power spectrum of $h(\cdot)$, $P_h(\vec{k})$, is from equation 3.5.

Following the same idea for the near junction potential solution, we obtain the mean energy far away from the junction as a function of z :

$$\langle E \rangle = q \cdot \{ E[\Phi_0] + E[\in \Phi_1] \} = q \cdot \left[V_0 e^{-\sqrt{\frac{q^2 N_D}{\varepsilon kT}} z} \right] \qquad (5.27)$$

The variance in the tangential plane as a function of z far away from the junction is:

$$Var[E] = q \cdot Var[\in \Phi_1] = q \cdot G_{\in\Phi_1}(0) = q \cdot \int_{0<|\vec{k}|<k_C} P_{\in\Phi_1}(\vec{k}) d\vec{k}, \qquad (5.28)$$

where the power spectrum of Φ_1 is:

$$P_{\in\Phi_1}(\vec{k}) = P_h(\vec{k}) \cdot \left| \left(V_0 \sqrt{\frac{q^2 N_D}{\varepsilon kT}} \right) e^{-\sqrt{K^2 + \frac{q^2 N_D}{\varepsilon kT}} z} \right|^2 . \qquad (5.29)$$

In Figures 1-4, we plot the standard deviation in the tangential plane as a function of distance away from the metal/organic interface normalized to the depletion width. Figures 1 and 3 are plots of the standard deviation near the junction where the potential is relatively large. Figures 2 and 4 are plots of the standard deviation far away from the junction where the potential is relatively small. The difference between Figures 1 and 3 and Figures 2 and 4 is only in the value we use for the charge density N_D. As we lower the charge density, the depletion width z_d increases but the standard deviation σ decreases.
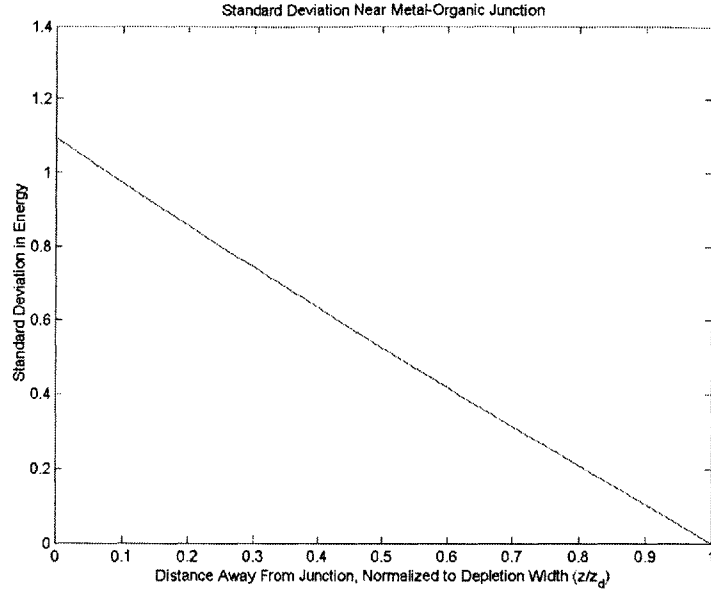
29

Figure 1: Standard deviation near the metal/organic junction calculated from the large potential approximation (equation 5.25). The values used were: $N_D = 10^{26} \, m^{-3}$, $w = 1 \, nm$, $\xi = 0.1 \, nm$, and $\alpha = 0.78$. Depletion width $z_d \approx 2 \, nm$.

Figure 2: Standard deviation far away from the metal/organic junction calculated from the small potential approximation (equation 5.28). The values used were: $N_D = 10^{26} \, m^{-3}$, $w = 1 \, nm$, $\xi = 0.1 \, nm$, $\alpha = 0.78$, and $T = 300°K$. Depletion width $z_d \approx 2 \, nm$.

Figure 3: Standard deviation near the metal/organic junction calculated from the large potential approximation (equation 5.25). The values used were: $N_D = 10^{25} \ m^{-3}$, $w = 1 \ nm$, $\xi = 0.1 \ nm$, and $\alpha = 0.78$. Depletion width $z_d \approx 6 \ nm$.
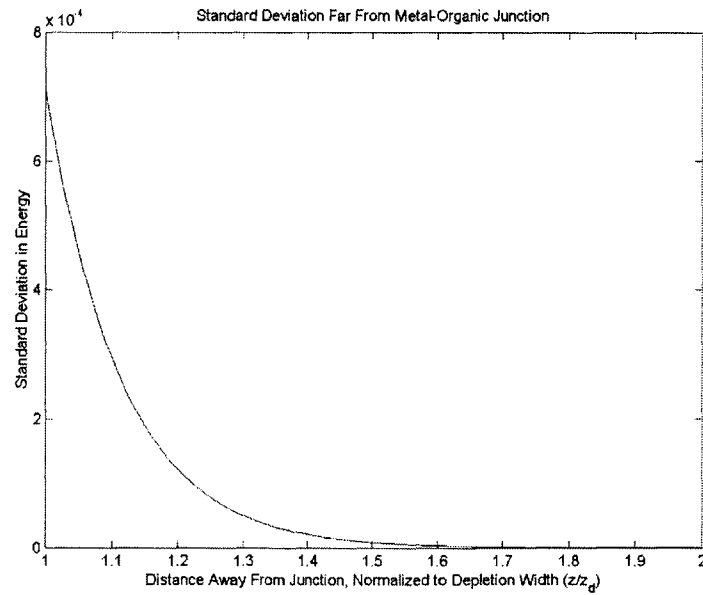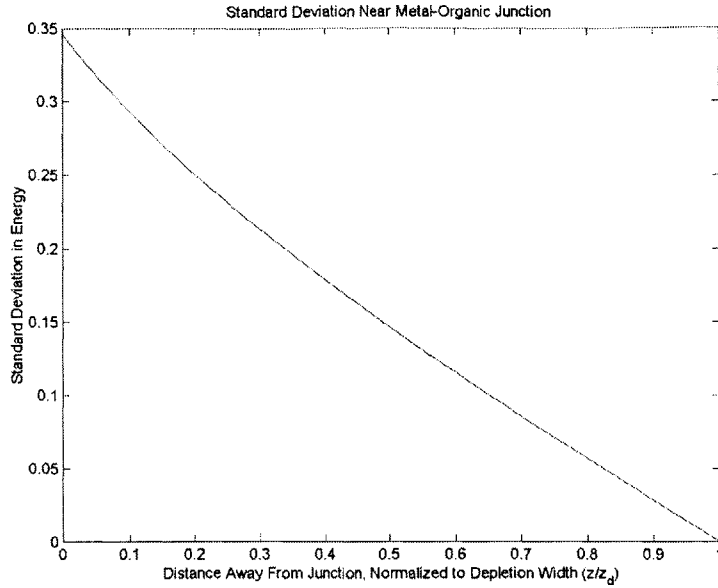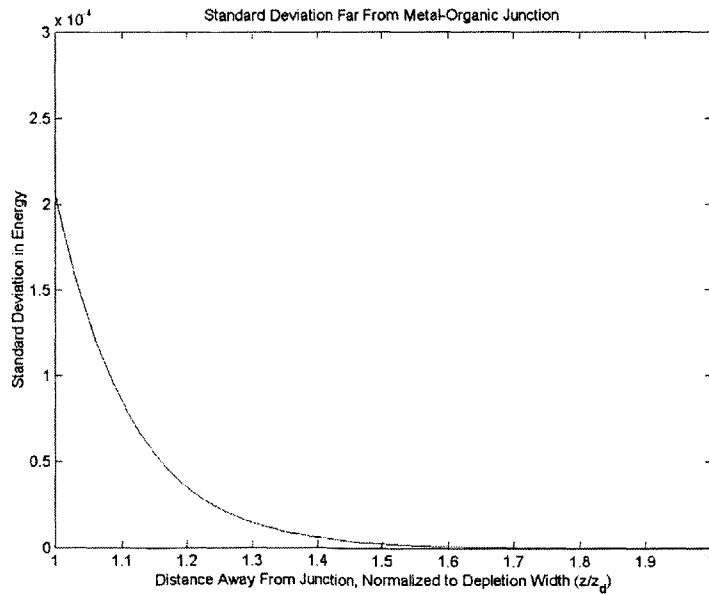

Figure 4: Standard deviation far away from the metal/organic junction calculated from the small potential approximation (equation 5.28). The values used were: $N_D = 10^{25} \ m^{-3}$, $w = 1 \ nm$, $\xi = 0.1 \ nm$, $\alpha = 0.78$, and $T = 300°K$. Depletion width $z_d \approx 6 \ nm$.

31

Chapter 6

Conclusions

In conclusion, we find that the electrostatic potential formed in the bulk will have a variance due to the roughness of the interface between the metal and organic semiconductor. This study on the broadening of energy, or density of states, near the interface is crucial in understanding interface-limited charge transport.[45] The calculation of charges hopping out of the broad density of states at the interface into the bulk using Marcus rates is shown in the appendix. The charges hop out of a broad Gaussian distribution of energy states at the interface to a much narrower Gaussian distribution in the bulk.[45]

A problem that we may improve on is the use of equations 4.3 and 4.4 for the expression of the charge density in the organic. This expression is valid for a non-degenerate inorganic semiconductor that has all its donors ionized with a position independent concentration N_D. A solution to this problem that may be more applicable to our case of organic semiconductors is to first assume that the depletion width is of length a_0 (average distance between organic molecules). Therefore, the depletion region is fixed to be only in the first organic layer. The amount of charge that moves out from the interface layer to the metal is determined by the applied voltage and measured built-in voltage. To find an expression relating the charge density in the interfacial layer and the voltage in the organic, we start out with the expression for capacitance:

$$C = \frac{Q}{V} \Leftrightarrow \frac{\varepsilon A}{d} = \frac{qN}{V} \Leftrightarrow \frac{\varepsilon V}{d} = q\sigma,$$

where C is the capacitance, Q is total charge, V is voltage, ε is permittivity, A is area, d is the distance where the voltage is across, q is the elementary charge, N is the total charge, σ and is the charge per unit surface area. The charge density in the depletion region is given by:

$$n = \frac{\varepsilon V_{bi}}{q a_0^{\,2}} + \frac{\varepsilon V_A}{q a_0 d_T},$$

where n is the charge density, V_{bi} is the built-in voltage across the depletion region, V_A is the applied voltage across the whole device, a_0 is the thickness of the depletion region (one layer in the organic), and d_T is the thickness of the device. Note that the second term will not contribute much for applied voltages around 10 to 20 V and for a device thickness of about 1000 Å with $a_0 \approx 10$ Å.

The solution for the potential will be similar to the full-depletion approximation except that we fix the depletion region to be one layer thick and our depletion region is not fully-depleted.

Chapter 7

Appendix

We calculate the current from the rate of charges hopping out of the interfacial layer into the bulk. The density of states in the interfacial layer will have a Gaussian distribution with standard deviation σ_I and a total capacity of N_I. The expression for the rate of charges hopping into the bulk out of the interfacial layer is:

$$\left[\frac{a_0 q N_I}{2\pi\sigma_I\sigma_B}\right] \int_{-\infty}^{\infty}\int_{-\infty}^{\infty} \frac{e^{-\frac{1}{2}\left(\frac{E_I}{\sigma_I}\right)^2}}{1+e^{\frac{E_I-E_F}{kT}}} e^{-\frac{1}{2}\left(\frac{E_B}{\sigma_B}\right)^2} e^{-\frac{(E_I-E_B-\lambda-\Delta)^2}{4\lambda kT}} dE_I dE_B \,,$$

where E_I and E_B are the energies of the transport sites in the interfacial layer and bulk layer, respectively, σ_B is the standard deviation of the bulk Gaussian distribution of states, E_F is the Fermi level, k is Boltzmann's constant, T is temperature, a_0 is the average distance between organic layers, q is the elementary charge, λ is the reorganization energy between two organic molecules, and $\Delta = a_0 q F$ is the energy shift of the bulk density of states due to an applied field F. Note that the last exponential expression in the integrand is the Marcus hopping rate. Using the Fermi distribution, we know the probability of which energy states are occupied in the interfacial layer given a Fermi level E_F. We multiply this by the rate of it hopping into an assumed-to-be completely empty bulk layer. Integrating this will give us the current density of interface-limited charge transport. We start solving the expression:

$$= \left[\frac{a_0 q N_I}{2\pi\sigma_I\sigma_B}\right] \int_{-\infty}^{\infty} \frac{e^{-\frac{1}{2}\left(\frac{E_I}{\sigma_I}\right)^2}}{1+e^{\frac{E_I-E_F}{kT}}} e^{-\frac{(E_I-\lambda-\Delta)^2}{4\lambda kT}} \int_{-\infty}^{\infty} e^{-\frac{1}{2}\left(\frac{E_B}{\sigma_B}\right)^2} e^{-\frac{E_B{}^2}{4\lambda kT}} e^{\frac{2E_I E_B}{4\lambda kT}} e^{-\frac{2E_B(\lambda+\Delta)}{4\lambda kT}} dE_B dE_I$$

$$note: \int_{-\infty}^{\infty} e^{-ax^2+bx} dx = \sqrt{\frac{\pi}{a}} e^{\frac{b^2}{4a}}$$

$$= \left[\frac{a_0 q N_I}{2\pi\sigma_I\sigma_B} \sqrt{\frac{\pi\left(4\sigma_B{}^2\lambda kT\right)}{\left(2\lambda kT+\sigma_B{}^2\right)}}\right] \int_{-\infty}^{\infty} \frac{e^{-\frac{1}{2}\left(\frac{E_I}{\sigma_I}\right)^2}}{1+e^{\frac{E_I-E_F}{kT}}} e^{-\frac{(E_I-\lambda-\Delta)^2}{4\lambda kT}} e^{\frac{\left(EI-(\lambda+\Delta)\right)^2 \sigma_B{}^2}{\left(2\lambda kT+\sigma_B{}^2\right)\left(4\lambda kT\right)}} dE_I$$

$$= \left[\frac{a_0 q N_I}{2\pi\sigma_I\sigma_B} \sqrt{\frac{\pi\left(4\sigma_B{}^2\lambda kT\right)}{\left(2\lambda kT+\sigma_B{}^2\right)}}\right] \int_{-\infty}^{\infty} \frac{1}{1+e^{\frac{E_I-E_F}{kT}}} e^{-\frac{(E_I-\lambda-\Delta)^2}{2\left(2\lambda kT+\sigma_B{}^2\right)}} e^{-\frac{1}{2}\left(\frac{E_I}{\sigma_I}\right)^2} dE_I$$

We've reduced the double integral to a single integral. This single integral can be split up into two regions, $-\infty < E_I \leq E_F$ and $E_F \leq E_I < \infty$. Note that the second region represents the charges above the Fermi level hopping into the bulk. We note that for high enough temperatures, this second region will dominate, and we can approximate the integral as being contributed mainly from this region. For low enough temperatures, this is no longer the case. The contribution of the second region approaches zero (as the Fermi distribution approaches a step function), and our integral will be mainly contributed from the first region, or the low temperature region. Let's first solve the expression in the second region, or the high temperature region:

HIGH T:

$$\approx \left[\frac{a_0 q N_I}{2\pi\sigma_I\sigma_B} \sqrt{\frac{\pi\left(4\sigma_B{}^2\lambda kT\right)}{\left(2\lambda kT+\sigma_B{}^2\right)}}\right] \int_{E_F}^{\infty} e^{-\frac{(E_I-E_F)}{kT}} e^{-\frac{(E_I-\lambda-\Delta)^2}{2\left(2\lambda kT+\sigma_B{}^2\right)}} e^{-\frac{1}{2}\left(\frac{E_I}{\sigma_I}\right)^2} dE_I$$

$$Note: -ax^2+bx = -a\left(x-\frac{b}{2a}\right)^2 + \frac{b^2}{4a}$$

$$\Rightarrow \mu = \frac{b}{2a} = -\left(\frac{(\lambda-\Delta)kT+\sigma_B{}^2}{2\lambda kT+\sigma_B{}^2+\sigma_I{}^2}\right)\left(\frac{\sigma_I{}^2}{kT}\right) \approx -\left((\lambda-\Delta)+\frac{\sigma_B{}^2}{kT}\right)$$

For $E_F \ll -\left((\lambda - \Delta) + \dfrac{\sigma_B{}^2}{kT}\right) = E_0$,

$$\approx \left[\frac{a_0 q N_I}{2\pi\sigma_I \sigma_B}\sqrt{\frac{\pi\left(4\sigma_B{}^2 \lambda kT\right)}{\left(2\lambda kT + \sigma_B{}^2\right)}}\right] e^{\frac{E_F}{kT}} e^{-\frac{(\lambda+\Delta)^2}{2\left(2\lambda kT+\sigma_B{}^2\right)}} \sqrt{\frac{2\pi\sigma_I{}^2\left(2\lambda kT+\sigma_B{}^2\right)}{\left(2\lambda kT+\sigma_B{}^2+\sigma_I{}^2\right)}} e^{\frac{\sigma_I{}^2\left((\lambda-\Delta)kT+\sigma_B{}^2\right)^2}{2k^2T^2\left(2\lambda kT+\sigma_B{}^2+\sigma_I{}^2\right)\left(2\lambda kT+\sigma_B{}^2\right)}}$$

We simplify the expression and make the approximation that σ_B is much smaller than σ_I, i.e., the Gaussian distribution in the bulk is much narrower than in the interface:

$$\approx \left[\frac{a_0 q N_I}{\sigma_I}\sqrt{(2\lambda kT)}\right] e^{\frac{E_F}{kT}} e^{\frac{(\lambda-\Delta)\sigma_B{}^2}{kT\left(2\lambda kT+\sigma_B{}^2\right)}} e^{\frac{\sigma_B{}^4}{2k^2T^2\left(2\lambda kT+\sigma_B{}^2\right)}}$$

Notice that the contribution from the high temperature region will go to zero as E_0 goes to negative infinity ($T \to 0$). When the contribution from the high temperature region becomes negligible to the contribution from the region $-\infty < E_I \le E_F$, we enter the low temperature regime:

LOW T: (use when high T approx goes to zero, i.e., E_F is no longer smaller than E_0)

$$\approx \left[\frac{a_0 q N_I}{2\pi\sigma_I \sigma_B}\sqrt{\frac{\pi\left(4\sigma_B{}^2 \lambda kT\right)}{\left(2\lambda kT + \sigma_B{}^2\right)}}\right] \int_{-\infty}^{E_F} e^{-\frac{(E_I-\lambda-\Delta)^2}{2\left(2\lambda kT+\sigma_B{}^2\right)}} e^{-\frac{1}{2}\left(\frac{E_I}{\sigma_I}\right)^2} dE_I$$

$$\approx \left[\frac{a_0 q N_I}{2\pi\sigma_I \sigma_B}\sqrt{\frac{\pi\left(4\sigma_B{}^2 \lambda kT\right)}{\left(2\lambda kT + \sigma_B{}^2\right)}}\right] e^{-\frac{(\lambda+\Delta)^2}{2\left(2\lambda kT+\sigma_B{}^2\right)}} e^{\frac{\sigma_I{}^2(\lambda+\Delta)^2}{2\left(2\lambda kT+\sigma_B{}^2\right)\left(2\lambda kT+\sigma_B{}^2+\sigma_I{}^2\right)}} \times$$

$$\frac{e^{-\left(\frac{2\lambda kT+\sigma_B{}^2+\sigma_I{}^2}{2\sigma_I{}^2\left(2\lambda kT+\sigma_B{}^2\right)}\right)\left(E_F-\left(\frac{\sigma_I{}^2(\lambda+\Delta)}{2\lambda kT+\sigma_B{}^2+\sigma_I{}^2}\right)\right)^2}}{\left(\dfrac{2\lambda kT+\sigma_B{}^2+\sigma_I{}^2}{\sigma_I{}^2\left(2\lambda kT+\sigma_B{}^2\right)}\right)\left(E_F-\left(\dfrac{\sigma_I{}^2(\lambda+\Delta)}{2\lambda kT+\sigma_B{}^2+\sigma_I{}^2}\right)\right)}$$

36

$$= \left[\frac{a_0 q N_I}{2\pi \sigma_I \sigma_B} \sqrt{\frac{\pi\left(4\sigma_B^2 \lambda kT\right)}{\left(2\lambda kT + \sigma_B^2\right)}} \right] \frac{e^{-\frac{(\lambda+\Delta)^2}{2\left(2\lambda kT+\sigma_B^2\right)}} e^{-\left(\frac{2\lambda kT+\sigma_B^2+\sigma_I^2}{2\sigma_I^2\left(2\lambda kT+\sigma_B^2\right)}\right)\left(E_F^2 - 2E_F\left(\frac{\sigma_I^2(\lambda+\Delta)}{2\lambda kT+\sigma_B^2+\sigma_I^2}\right)\right)}}{\left(\frac{2\lambda kT+\sigma_B^2+\sigma_I^2}{\sigma_I^2\left(2\lambda kT+\sigma_B^2\right)}\right)\left(E_F - \left(\frac{\sigma_I^2(\lambda+\Delta)}{2\lambda kT+\sigma_B^2+\sigma_I^2}\right)\right)}$$

Again, simplifying the expression, we obtain:

$$= \left[\frac{a_0 q N_I}{\sigma_I} \sqrt{\frac{\lambda kT}{\pi\left(2\lambda kT+\sigma_B^2\right)}} \right] \frac{e^{-\left(\frac{1}{2\left(2\lambda kT+\sigma_B^2\right)}\right)\left(E_F-(\lambda+\Delta)\right)^2}}{\left(\frac{1}{2\lambda kT+\sigma_B^2}\right)\left(E_F-(\lambda+\Delta)\right)}$$

In conclusion, we have a critical energy $E_0 = -\left((\lambda-\Delta)+\frac{\sigma_B^2}{kT}\right)$ that determines the

separation between the high and low temperature regimes.

References

1. F.-J. Meyer zu Heringdorf *et al.*, Nature (London) **412**, 517 (2001).
2. A.C. Dürr, F. Schreiber, K.A. Ritley, V. Kruppa, J. Krug, H. Dosch, and B. Struth, Phys. Rev. Lett. **90**, 016104 (2003).
3. Y.-P. Zhao, J.B. Fortin, G. Bonvallet, G.-C. Wang, and T.-M. Lu, Phys. Rev. Lett. **85**, 3229 (2000).
4. F. Biscarini, P. Samorí, O. Greco, and R. Zamboni, Phys. Rev. Lett. **78**, 2389 (1997).
5. G. Palazantzas and J. Krim, Phys. Rev. Lett. **73**, 3564 (1994).
6. B.B. Mandelbrot, *The Fractal Geometry of Nature* (Freeman, New York, 1982).
7. Y. Zhao, G.-C. Wang, and T.-M. Lu, *Experimental Methods in the Physical Sciences: Volume 37 -- Characterization of Amorphous and Crystalline Rough Surface: Principles and Applications* (Academic Press, New York, 2001).
8. E. Schlömann, J. Appl. Phys. **41**, 1617 (1970).
9. Q. Jiang, H.-N. Yang, and G.-C. Wang, Surf. Sci. **373**, 181 (1997).
10. G. Palasantzas and J. Barnás, Phys. Rev. B **56**, 7726 (1997).
11. G.A. Farias and A.A. Maradudin, Phys. Rev. B **28**, 5675 (1983).
12. M. Leyva-Lucero, E.R. Méndez, T.A. Leskova, A.A. Maradudin, and J.Q. Lu, Opt. Lett. **21**, 1809 (1996).
13. K.A. O'Donnell and R. Torre, Opt. Commun. **138**, 341 (1997).
14. *The Fractal Approach to Heterogeneous Chemistry: Surfaces, Colloids, Polymers*, edited by D. Avnir (Wiley, New York, 1989).
15. M. Saillard and D. Maystre, J. Opt. Soc. Am. A **7**, 982 (1990).
16. J.-J. Greffet, Opt. Lett. **17**, 238 (1992).
17. R.I. Hedge, M.A. Chonko, and P.J. Tobin, J. Vac. Sci. Technol. B **14**, 3299 (1996).
18. T. Clausen and O. Leistiko, Semicond. Sci. Technol. **10**, 691 (1995).
19. F. Ladouceur, J. Lightwave Technol. **15**, 1020 (1997).
20. W.A. Gardner, *Introduction to Random Processes with Applications to Signals and Systems, 2nd Edition* (McGraw-Hill, Inc., New York, 1990).
21. T. Assefi, *Stochastic Processes and Estimation: Theory with Applications* (Wiley, New York, 1979).
22. Dynamics of Fractal Surfaces , edited by F. Family and T. Viscek (World Scientific, Singapore, 1991).
23. T. Viscek, *Fractal Growth Phenomena* (World Scientific, Singapore, 1992).

24. A.-L. Barabási and H.E. Stanley, *Fractal Concepts in Surface Growth* (Cambridge University Press, New York, 1995).

25. P. Meakin, *Fractals, Scaling, and Growth Far from Equilibrium* (Cambridge University Press, Cambridge, 1998).

26. G. Palasantzas, Phys. Rev. B **48**, 14472 (1993); **49**, 5785 (1994).

27. G. Palasantzas, J. Appl. Phys. **81**, 246 (1997).

28. G. Palasantzas, J. Appl. Phys. **82**, 351 (1997).

29. G. Palazantzas and G.M.E.A. Blackx, J. Appl. Phys. **92**, 7175 (2002).

30. G. Palazantzas and G.M.E.A. Blackx, J. Chem. Phys. **118**, 4631 (2003).

31. G. Palasantzas and J.Th.M. De Hosson, J. Appl. Phys. **93**, 898 (2003).

32. Y.-P. Zhao, R.M. Gamache, G.-C. Wang, T.-M. Lu, G. Palasantzas, and J.Th.M. De Hosson, J. Appl. Phys. **89**, 1325 (2001).

33. Y.-P. Zhao, G.-C. Wang, and T.-M. Lu, Phys. Rev. B. **55**, 13938 (1997).

34. R.C. Munoz, R. Finger, C. Arenas, G. Kremer, and L. Moraga, Phys. Rev. B. **66**, 205401 (2002).

35. J.D. Jackson, *Classical Electrodynamics, 3rd Edition* (John Wiley & Sons, Inc., New York, 1999).

36. S.M. Sze, *Physics of Semiconductor Devices, 2nd Edition* (John Wiley & Sons, Inc., New York, 1981).

37. T.S. Rahman and A.A. Maradudin, Phys. Rev. B. **21**, 504 (1980).

38. L.I. Daikhin, A.A. Kornyshev, and M. Urbakh, Phys. Rev. E. **53**, 6192 (1996).

39. L.I. Daikhin, A.A. Kornyshev, and M. Urbakh, J. Chem. Phys. **108**, 1715 (1998).

40. A.H. Nayfeh, *Perturbation Methods* (John Wiley & Sons, Inc., New York, 1973).

41. S.S. Haykin, *Communication Systems, 4th Edition* (John Wiley & Sons, Inc., New York, 2000).

42. C.W. Tang and S.A. VanSlyke, Appl. Phys. Lett. **51**, 913 (1987).

43. C.W. Tang, S.A. VanSlyke, and C.H. Chen, J. Appl. Phys. **65**, 3610 (1989).

44. J.R. Sheats, H. Antoniadis, M. Hueschen, W. Leonard, J. Miller, R. Moon, D. Roitman, and A. Stocking, Science **273**, 884 (1996).

45. M.A. Baldo and S.R. Forrest, Phy. Rev. B **64**, 8 (2001).